JOURNAL OF Applied Polymer SCIENCE

Measurement of thermal conductivity of epoxy resins during cure

G. Struzziero [1], B. Remy,[2] A. A. Skordos [3]
[1]Faculty of Aerospace, Structural Integrity & Composites, Delft University of Technology, Delft 2628 CD, Netherlands
[2]Cytec Solvay group, Wrexham Clwyd LL13 9UZ, UK
[3]School of Aerospace, Transport and Manufacturing, Cranfield University, Bedford MK43 0AL, UK
Correspondence to: G. Struzziero (E-mail: g.struzziero@tudelft.nl). Tel: + 31 (0) 152781215.

ABSTRACT: This work reports the development of a methodology for the measurement of thermal conductivity of thermosetting polymers during their cure. The study addresses the reliability and robustness of the method through FEA modeling and testing using a noncuring material with known thermal conductivity. The thermal conductivity and its evolution during the cure has been measured for three widely used aerospace epoxy resins, namely, RTM6, 890RTM, and the XU3508/XB3473 system as function of cure temperature. A constitutive model expressing the dependence of thermal conductivity on the degree of cure and temperature has been established. The device developed here can measure thermal conductivity of epoxy resin with accuracy up to 3%. © 2018 The Authors. Journal of Applied Polymer Science published by Wiley Periodicals, Inc. J. Appl. Polym. Sci. **2019**, *136*, 47015.

Received 15 May 2018; accepted 8 July 2018
DOI: 10.1002/app.47015

INTRODUCTION

The cure of carbon fiber-reinforced composites is a key aspect of the manufacturing of advanced composites. The capability to analyze the cure process can lead to process designs that combine high efficiency with elimination of process defects. An accurate model of the heat transfer phenomena occurring during the cure is necessary for this type of analysis. The complex behavior of a thermosetting matrix during the cure process, which undergoes transformations through different states from an oligomeric liquid to a solid glass, is incorporated in simulations of this type through constitutive models. These include models of the cure kinetics and thermal properties, such as specific heat and thermal conductivity, expressing the evolution of material behavior as a function of temperature and the degree of cure.

An accurate measurement of thermal conductivity evolution is necessary in the context of heat transfer analysis to produce the corresponding constitutive model. Measurement techniques can be classified into two main categories: steady-state and transient methods. Among steady-state methods, the hot-guarded plate technique is used for the determination of thermal conductivity of low-conductivity materials. This technique, which is standardized in ISO 8302:1991 and ASTM C177-04, has been used successfully to measure the conductivity of partially cured samples in the solid state.[1–3] Transient techniques, based on the application of periodic heating of the sample and the measurement of the phase lag in the periodic signals, have been utilized to estimate the thermal diffusivity of preimpregnated epoxy fiber material during the cure using a planar geometry.[4,5] Efforts have also been made to use differential scanning calorimetry (DSC) to measure thermal conductivity of liquid polymers.[6–9] However, this method can only provide results for a given degree of cure and while the material is not curing. Some transient methods determine thermal conductivity by recording the change in temperature as function of time after a pulse of heating. The laser flash method, which is standardized in ASTM E1461-13, has been applied to measure the thermal conductivity of thermosetting materials and their prepregs as a function of temperature[10–12] and also as a function of the degree of cure.[13] The transient hot-wire method, standardized in ASTM D5930-09, has also been utilized to determine the thermal conductivity of polymers in the molten and solid state and of diffusivity as function of temperature.[14–17] Thermal conductivity has also been estimated through inverse scheme solutions using information from monitoring of the cure process and simulation. [18,19] These techniques partially address the issue of measuring the thermal conductivity of thermosets during cure. The majority are not appropriate for operation during the cure, whereas the two methods that can be used during the cure (laser flash and periodic heating of planar samples) work well for geometries that involve low thickness and large in-plane dimensions to allow accurate application of the 1D assumption necessary for the associated analysis. This geometrical constraint focuses on the applicability of these methods to preimpregnated composites and resin films, whereas use with neat low-viscosity epoxies appropriate for liquid molding is problematic.

This work reports the development of an experimental setup that allows measurement of thermal conductivity of the curing material in a cylindrical container. This setup allows use of the method throughout different material states, from a very low viscosity liquid to a glassy solid. A heat transfer model of the setup has been built to verify the validity of the results, investigate the influence of experimental parameters, and establish the sensitivity of the measurement method. Measurements for an inert liquid and three widely used aerospace epoxy resins have been carried out. The analysis of measurements for the epoxy materials has been performed using cure kinetics and specific heat capacity models developed based on calorimetry results. The thermal conductivity evolution results obtained in the form of constitutive models has been developed for the three epoxy systems of this study.

METHODS

Thermal Conductivity Measurement Apparatus and Principle

The device designed to perform the measurement comprises a copper block with cooling fins and a cylindrical hole in its center designed to host a hollow copper tube of 3.5 mm in radius with a wall thickness of 1 mm and a height of 40 mm. The device is illustrated in Figure 1.

The liquid resin is poured in the copper tube, which is then closed with a cork. The cork has an opening in its center to allow a centrally placed thermocouple to reach the resin and also to ensure central positioning in the tube. The copper tube is then inserted in the cylindrical hole of the copper block. Two insulating plates made of Sindanyo are placed on the top and lower sides of the copper block. A flexible heating cord (Omega HTC, Manchester, UK) is wound around the cooling fins. The copper block temperature is controlled by a Eurotherm controller (808), which regulates the power across the heating cord. A periodic temperature profile is imposed to the copper block. Because of the thermal inertia of the resin, the temperature measured at the center of the resin region follows a periodic profile with a phase lag. An example of the periodic signal of the resin and copper temperature is reported in Figure 2.

The periodic heat transfer problem formulated accepts a steady periodic solution, which expresses the temperature as a function of radial position (r) and time (t) as follows[20]:

$$T(r,t) = A\,\mathrm{Real}\left\{\frac{I_0\left(r\sqrt{i\,\omega\,\rho\,c_p/K}\right)}{i\,I_0\left(r_0\sqrt{i\,\omega\,\rho\,c_p/K}\right)}e^{i\,(\omega\,t)}\right\} \tag{1}$$

where ω is the angular frequency of the temperature modulation, A is the amplitude of the modulation, ρ is the instantaneous resin density, r_0 is the inner radius of the copper tube, c_p the instantaneous specific heat capacity of the resin, K is the thermal conductivity of the resin, and I_0 is the modified Bessel function of zero order expressed as:

$$I_0\left(z\sqrt{i}\right) = ber(z) + ibei(z) \tag{2}$$

where

$$ber(z) = \sum_{n=0}^{\infty}\frac{(-1)^n\left(\frac{1}{4}z^2\right)^{2n}}{(2n)!^2} \tag{3}$$

$$bei(z) = \sum_{n=0}^{\infty}\frac{(-1)^n\left(\frac{1}{4}z^2\right)^{2n+1}}{(2n+1)!^2} \tag{4}$$

The solution at the center of the cylindrical copper tube is

$$T(0,t) = A\,\mathrm{Real}\left\{\left[ber\left(r_0\sqrt{\omega\,\rho\,c_p/K}\right) - bei\left(r_0\sqrt{\omega\,\rho\,c_p/K}\right)\right]^{-1}e^{i\,(\omega\,t)}\right\} \tag{5}$$

or

$$T(0,t) = M\sin\left(\omega\,t - \phi\right) \tag{6}$$

where

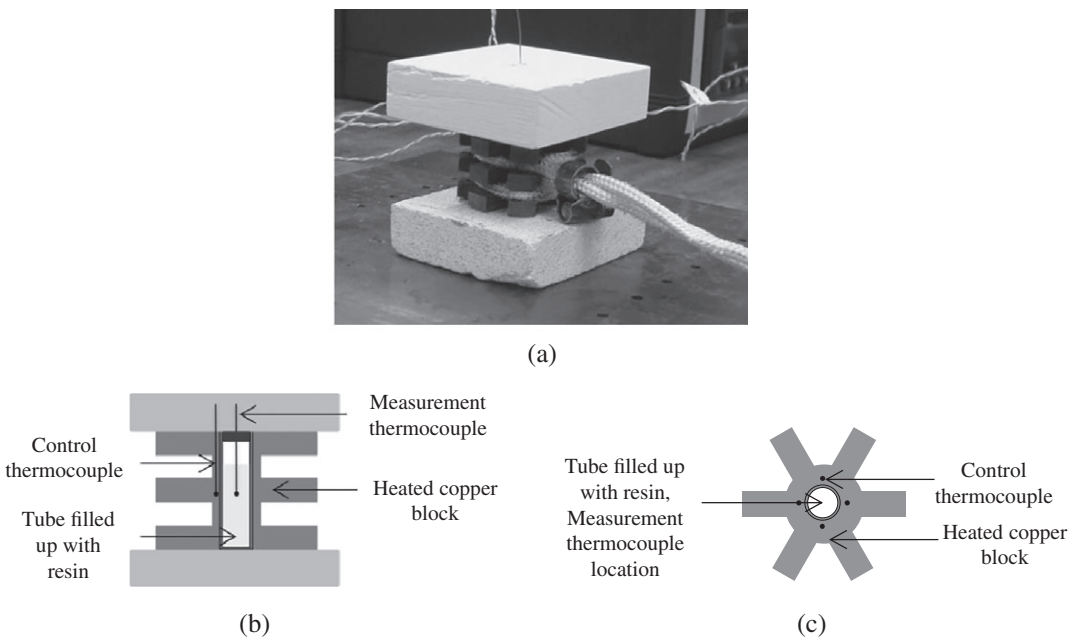

Figure 1. . (a) Experimental apparatus. (b) Cross section. (c) Top view.

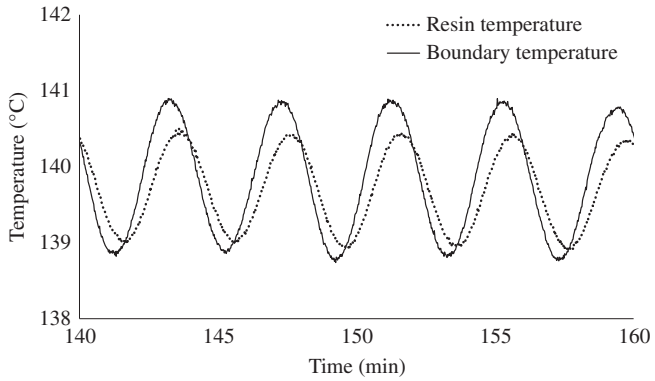

Figure 2. Temperature profile at the boundary and at the center of the resin region.

$$M = \frac{A}{\sqrt{\left(ber\left(r_0\sqrt{\omega\,\rho\,c_p/K}\right)\right)^2 + \left(bei\left(r_0\sqrt{\omega\,\rho\,c_p/K}\right)\right)^2}} \quad (7)$$

and

$$\phi = \tan^{-1}\left(\frac{bei\left(r_0\sqrt{\omega\,\rho\,c_p/K}\right)}{ber\left(r_0\sqrt{\omega\,\rho\,c_p/K}\right)}\right) \quad (8)$$

The argument $z = r_0\sqrt{\omega\,\rho\,c_p/K}$ in eq. (8) can be calculated from the measurement of the phase difference ϕ, and the thermal conductivity K can be estimated as:

$$K = \frac{{r_0}^2\,\omega\,\rho\,c_p}{z^2} \quad (9)$$

Materials

Glycerin, supplied by Sigma-Aldrich,[21] was used as a noncuring material to benchmark the method. The following epoxy resins were used: Hexcel RTM6,[22] a degassed, premixed, monocomponent resin specifically designed for resin transfer molding processes with service temperatures from −60 up to 120 °C; Cycom 890RTM,[23] a one-part liquid epoxy resin with low reactivity designed for infusion applications; and Huntsman XU3508/XB3473,[24] a two-component system using a liquid-toughened epoxy resin used in filament winding and pultrusion.

Methodology

Thermal conductivity measurements were carried out at two isothermal temperatures for RTM6 and 890RTM and three temperatures for XU350/XB3473. Three identical tests were run for each condition. The test temperatures for RTM6 were 137 and 156 °C, those for 890RTM were 154 and 175 °C, and those for XU3508/XB3473 were 91, 111, and 130 °C. Tests with glycerin were carried out at 40 and 100 °C. The modulation applied to the boundary temperature applied had an amplitude equal to 1 °C and a period equal to 4 min. The 4 min period constitutes a good trade-off between measurement accuracy and number of cycles per test. The thermocouples used in testing were calibrated before each run using the control thermocouple of the Eurotherm controller as a temperature reference. Before each test, the copper tube was filled with resin up to three quarters, closed with the cork seal, and placed in the copper block. Subsequently, the measurement thermocouple, which has a rigid probe of 0.5 mm in diameter, was passed through the central opening in the cork seal and held in place by it. The modulated boundary condition was applied to the copper using an in-house LabVIEW code interfacing the temperature controller and the measurement thermocouples with a desktop PC and acquiring the data of the experiment. The data obtained in the form of temperature time series were analyzed using an in-house Matlab procedure based on Fourier transform to evaluate the phase difference as a function of time. The Bessel argument in eq. (8) was calculated from this information, and thermal conductivity was estimated using eq. (9).

Cure characterization of the three resin systems was carried out using a TA Instruments Q200 Differential Scanning Calorimeter. One dynamic experiment at 2 °C/min and two isothermal DSC tests at 160 and 180 °C were carried out for RTM6. Similarly, a dynamic experiment at 2 °C/min and two isothermal DSC tests at 180 and 200 °C were carried out for 890RTM. One dynamic test at 1 °C/min and four isothermal tests at 90, 120, 160, and 200 °C were performed for the XU3508/XB3473 system.

Isothermal modulated DSC (MDSC) experiments were carried out using a TA Instruments Q200 calorimeter to measure the specific heat capacity of the resin systems. For RTM6, the tests were carried out at 140 and 160 °C, those for 890RTM were carried out at 160 and 180 °C, and those for XU3508/XB3473 were carried out at 90, 120, and 160 °C. The frequency of the modulation was 1 cycle/min, and the amplitude was 1 °C. The glass-transition temperature evolution of the XU3508/XB3473 system was measured using 13 partially cured samples. The samples were heated at 1 °C/min up to increasing final temperatures. For the determination of T_{g_0}, the sample needs to be quickly cooled down to a temperature below T_{g_0}.

Subsequently, the partially cured samples were tested using MDSC at a 1 °C/min ramp rate, with a modulation set at 1 cycle/min and an amplitude of 1 °C, to identify the glass-transition temperature using the step in specific heat capacity observed.

Finite Element Modeling

A finite element (FE) model built and solved in MSC Marc[25] was utilized to investigate heat transfer effects in the measuring cell. Because of the axial symmetry in the z direction (Figure 3), the heat transfer problem can be described by an axisymmetric model.

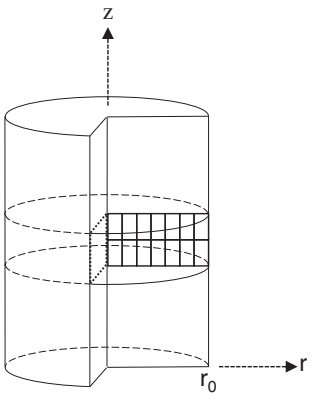

Figure 3. FE modeling domain.

The elements used are axisymmetric bilinear quadrilateral elements (element 40 in the Marc element library)[26] suitable for heat transfer analysis. This allowed representing the heart transfer problem domain as a rectangle with its length equal to the inner radius of the copper tube. Thermal material properties were defined through user-defined tables, whereas the cure kinetics and the temperature boundary condition were defined through user MSC Marc subroutines UCURE and FORCDT, respectively.[27] The periodic temperature boundary condition was applied to the nodes in contact with the inner wall of the copper tube at 3.5 mm from the center. Initial conditions were also defined for temperature and the degree of cure.

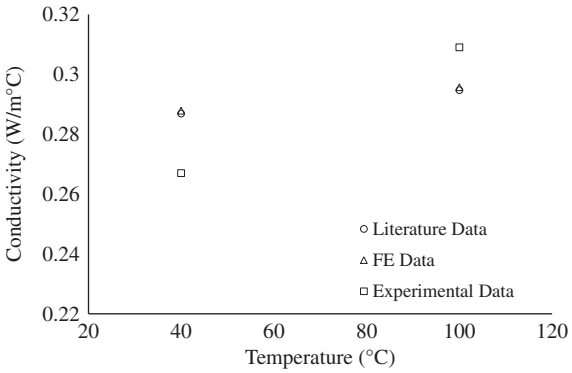

Figure 4. Thermal conductivity of glycerin.

RESULTS AND DISCUSSION

Verification and Sensitivity Analysis Using Glycerin

Experimental measurements and FE analyses were carried out for the case of glycerin to investigate the thermal response of the setup and to verify the data reduction procedure for a material with known material properties. Simulations were performed at two different temperatures (40 and 100 °C) to match the experimental tests. The amplitude of the periodic boundary condition was set at 1 °C, whereas the period was set at 4 min. Table I reports the thermal properties of glycerin used in the simulation. The values utilized are reported by van Gelder.[28] The results from simulations and tests are reported in Figure 4 alongside literature values.

The measured values of thermal conductivity show a deviation of about 8% in comparison to the literature. The comparison between FE results and literature values is carried out to verify the data reduction procedure and its implementation. The fact that the FE results are identical to the input literature values reflects the accuracy of the data reduction used for the calculation of thermal conductivity from the modulated temperature response.

A sensitivity analysis was undertaken to investigate the effect on accuracy of misplacing the central thermocouple. The analysis was carried out by altering the position at which temperature is acquired by 0.5–2 mm. The results are summarized in Figure 5.

It can be observed that the position of the thermocouple can play an important role in accuracy. Misplacing the thermocouple by 0.5 mm causes an overestimation of less than 0.01 W m^{-1} °C^{-1} (about 3%), whereas misplacing the thermocouple by 2 mm results in a deviation of about 0.16 W m^{-1} °C^{-1} (about 50%). These results indicate that the deviations observed in the glycerin measurement can be caused by a misplacement of about 0.75 mm for both the 40 °C and the 100 °C experiment. The results of the simulation show that there is no significant influence of temperature on the sensitivity to sensor misplacement.

Overall, these results show that the procedure utilized for the measurement and data reduction is appropriate. A positional accuracy of 0.5 mm is required to limit the measurement error to levels below 3%. This is achievable with the current configuration based on a rigid tip thermocouple, while a correction to account for the finite diameter of the tip is possible by considering a value for the radius considered in data reduction [r_0 in eq. (9)] decreased by the tip radius (0.25 mm). This correction is applied to the analysis of curing material tests reported in the following sections.

Resin Cure Kinetics, Specific Heat Capacity, and Density

The resin systems used in this study follow different cure kinetics behaviors. The cure kinetics of RTM6 is a combination of an *n*th order model and an autocatalytic model and is described as follows[29]:

$$\frac{d\alpha}{dt} = k_1 (1-\alpha)^{n_1} + k_2 (1-\alpha)^{n_2} \alpha^m \tag{10}$$

where α is the degree of cure. n_1, n_2, and m are reaction orders, and k_1 and k_2 are rate constants defined as follows:

$$k_i = \frac{1}{\frac{1}{k_{iC}} + \frac{1}{k_D}}, i = \{1,2\} \tag{11}$$

where k_{iC} describes the chemical component of the rate constant and can be defined as follows:

$$k_{iC} = A_i e^{\left(\frac{-E_i}{RT}\right)}, i = \{1,2\} \tag{12}$$

where T is the absolute temperature, A_i is the pre-exponential Arrhenius coefficient, E_i is the activation energy, and R is the universal gas constant. The diffusion process rate constant (k_D) is expressed as follows:

$$k_D = A_D e^{\left(\frac{-E_D}{RT}\right)} e^{\left(\frac{-b}{f(T-Tg)+g)}\right)} \tag{13}$$

Table I. Thermal Properties of Glycerin[28]

Temperature (°C)	Thermal conductivity (W m^{-1} °C^{-1})	Density (kg m^{-3})	Specific heat (J kg^{-1} °C^{-1})	Thermal diffusivity (10^{-6} m^2 s^{-1})
40	0.2869	1248.1	2458	0.0935
80	0.2921	1221.5	2625	0.0911
100	0.2947	1207.6	2687	0.0908

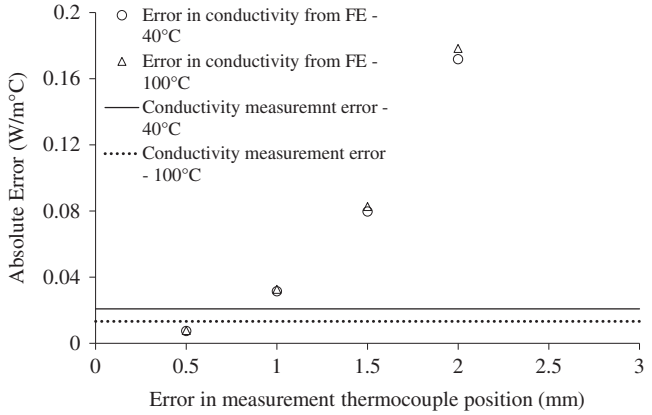

Figure 5. Sensitivity to thermocouple misplacement.

where A_D is the Arrhenius diffusion pre-exponential factor, E_D is the diffusion activation energy, and b, f, and g are constants.

The cure kinetics of the 890RTM is expressed by an autocatalytic model that includes an explicit diffusion[30]:

$$\frac{d\alpha}{dt} = \frac{Ae^{\left(\frac{-E}{RT}\right)}}{1+e^{C(\alpha-\alpha_C-\alpha_T T)}}(1-\alpha)^n \alpha^m \quad (14)$$

where α_C and α_T are coefficients governing the transition of the kinetics from chemical to diffusion control, respectively.

The XU3508/XB3473 resin system is modeled using the following expression involving an nth order reaction and an explicit term controlling diffusion:

$$\frac{d\alpha}{dt} = \frac{Ae^{\left(\frac{-E}{RT}\right)}}{1+e^{C(\alpha-\alpha_C-\alpha_T T)}}(1-\alpha)^n \quad (15)$$

The glass-transition temperature development is modeled using the Di Benedetto equation[31]:

$$T_g = T_{g_0} \frac{\left(T_{g_\infty} - T_{g_0}\right)\lambda\alpha}{1-(1-\lambda)\alpha} \quad (16)$$

T_{g_0} is the glass-transition temperature of the uncured material, T_{g_∞} is the glass-transition temperature of the fully cured material, and λ is a fitting parameter controlling the convexity of the dependence of glass-transition temperature on the degree of cure.

Experimental results and cure kinetics model fitting for the three resin systems are illustrated in Figure 6. For the characterization of the RTM6 and 890RTM epoxy system, only two isothermal temperatures have been selected to characterize the cure kinetics because the cure kinetics of these systems have been already addressed in the literature, whereas for the XU3508/XB3473 epoxy system, four isothermal temperatures have been chosen because this constitutes the first attempt to characterize its cure kinetics. Therefore, a higher number of isothermal temperatures were required. The isothermal temperatures were selected to be equidistant and considering the standard temperature at which the systems are cured. Table II reports the fitting parameters of the models.

The fitting parameters for the Di Benedetto equation for RTM6 and 890RTM can be found in the literature.[30,33] In the case of the XU3508/XB3473 system, the evolution of glass-transition temperature was quantified using partially cured samples and the corresponding cure kinetics model. Figure 7 illustrates the results and the corresponding fitting, which is very close to the experiment. The Di Benedetto equation fitting parameters for XU3508/XB3473 as well as the literature values for RTM6 and 890RTM[30,33] are reported in Table III.

Specific heat capacity values are required to estimate thermal conductivity using eq. (9). A model representing the evolution of the specific heat for the three different systems has been developed. This is as follows:

$$c_{pr} = C_{rub} + C_{rub\alpha}\alpha + C_{rubT}T + \frac{\left(C_{glass} + C_{glassT}T - C_{rub} - C_{rub\alpha}\alpha - C_{rubT}T\right)}{1+exp\left(C_w\left(T - T_g - \sigma - \sigma_T T\right)\right)} \quad (17)$$

where C_{rub} and C_{glass} are the intercepts in the rubber and glass state, respectively. $C_{rub\alpha}$ and C_{rubT} govern the dependence on the degree of cure and temperature in the rubber state, respectively. C_{glassT} is the dependence on temperature in the glass state, and σ, C_w, and σ_T are the parameters controlling the position, breadth, and temperature dependence of the rubber to glass transition, respectively.

The experimental specific heat capacity data alongside the model fitting are illustrated in Figure 8. The isothermal temperatures for the specific heat capacity characterization have been chosen to have enough data before the transition. The fitting parameters of the heat capacity model are reported in Table IV.

It can be observed that the model successfully reproduces the evolution of specific heat capacity for the three resin systems.

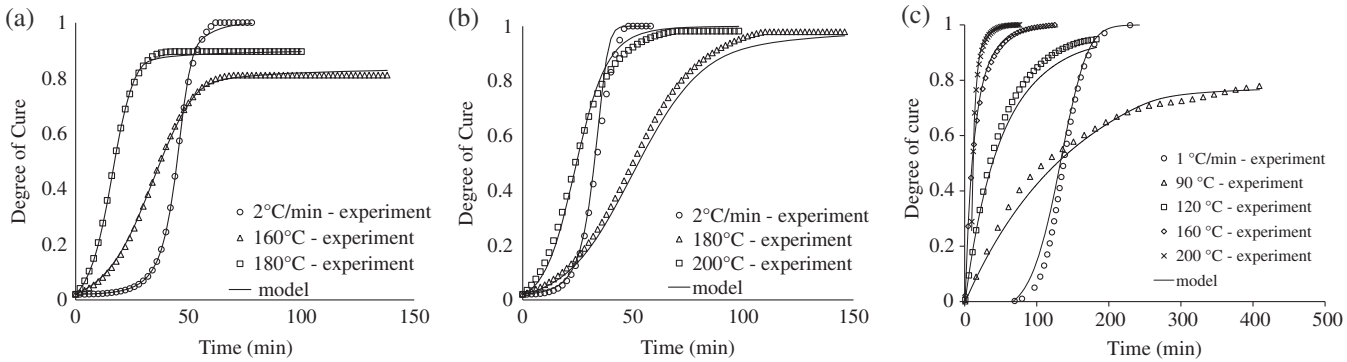

Figure 6. Comparison of cure kinetics model with experimental results for (a) RTM6, (b) 890RTM, and (c) XU3508/XB3473.

Table II. Cure Kinetics Fitting Parameters

RTM6		890RTM		XU3508/XB3473	
A_1 (s^{-1})	293 371.7	A (s^{-1})	219 270.4	A (s^{-1})	759
A_2 (s^{-1})	123 953	E (J mol^{-1})	72 357.21	E (J mol^{-1})	47 850
A_d (s^{-1})	1.21×10^{20}	n	1.11	n	1.25
E_1 (J mol^{-1})	81 495.77	m	0.87	C	80
E_2 (J mol^{-1})	64 231.31	C	28.53	α_C	0.17
E_d (J mol^{-1})	135 324	α_C	−3.73	α_T (K^{-1})	0.00631
n_1	3.96	α_T (K^{-1})	0.010	H_{tot} (J g^{-1})	250
n_2	1.61	H_{tot} (J g^{-1})	425		
m	1.15				
b	0.68				
H_{tot} (J g^{-1})	466				

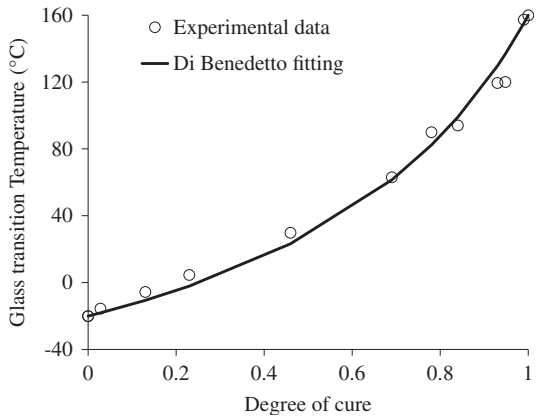

Figure 7. Di Benedetto model for the XU3508/XB3473 system.

Steps occurring at vitrification are replicated with high accuracy while the simulated plateau behavior is very close to what was observed in MDSC experiments.

The density evolution of the three resin system has been calculated based on the coefficient of thermal expansion in the rubber state and shrinkage evolution with the degree of cure as follows:

$$\rho_i = \frac{\rho_{i-1}}{1 + \alpha_{vr}\Delta T - \gamma\Delta\alpha} \tag{18}$$

where ρ_i and ρ_{i-1} are the density values at the current and previous time steps, respectively. α_{vr} is the volumetric coefficient of thermal expansion of the resin in the rubber state, and γ is the volumetric shrinkage coefficient. The values of coefficient of thermal expansion, shrinkage coefficient, and initial density for the three resins are reported in Table V.[22–24,32,34,35]

Table III. Di Benedetto Model Fitting Parameters[30,33]

	RTM6	890RTM	XU3508/XB3473
T_{g_0} (°C)	−11	−14	−20
T_{g_∞} (°C)	206	214	160
λ	0.435	0.396	0.371

Sensitivity Analysis and Thermal Conductivity for Curing Materials

The robustness of the reduction procedure expressed by eqs. (1)–(9) has been investigated using FE modeling. In this analysis, the thermal conductivity was considered constant and equal to 0.15 W m^{-1} °C^{-1}, and the periodic boundary condition had an amplitude of 1 °C and a period of 4 min. Two scenarios have been used for the 890RTM resin system: one involving no heat generation and the other including the curing reaction as expressed by the model in eq. (14) and the corresponding heat generation. Heat generation is computed in the FE models as the product of the reaction rate resulting from the cure kinetics model and the total enthalpy of the reaction measured by DSC and reported in Table II. The simulation and data reduction were carried out for three different temperatures (160, 180, and 200 °C). The results reported in Table VI show that the procedure developed is robust over the range of temperatures considered and with respect to exothermic effects as the percentage error in the calculated thermal conductivity is lower than 1.3% in all cases. This result confirms that the effect of the exothermic reaction and of nonlinearity of heat transfer phenomena to the measurement and associated estimations is negligible, making the setup suitable for use with materials of this type.

The influence of period on the sensitivity of thermal conductivity estimates on thermocouple misplacement was investigated for the case of curing materials. Periods of 1, 4, and 10 min were utilized in FE models to asses these effects. The results of this analysis are presented in Figure 9.

The sensitivity to misplacement of the temperature sensor decreases with increasing modulation period. This is explained by the proportional dependence of the conductivity estimate on angular frequency implied by eq. (9), which results in an inversely proportional dependence of conductivity sensitivity to radius with respect to period. In practical terms, this means that using longer period results in a more robust estimate; however, the selection of the period is limited by the requirement for a certain number of measurements during the experiment. The choice of a 4 min period in the tests carried out in this work presents an appropriate compromise between these two.

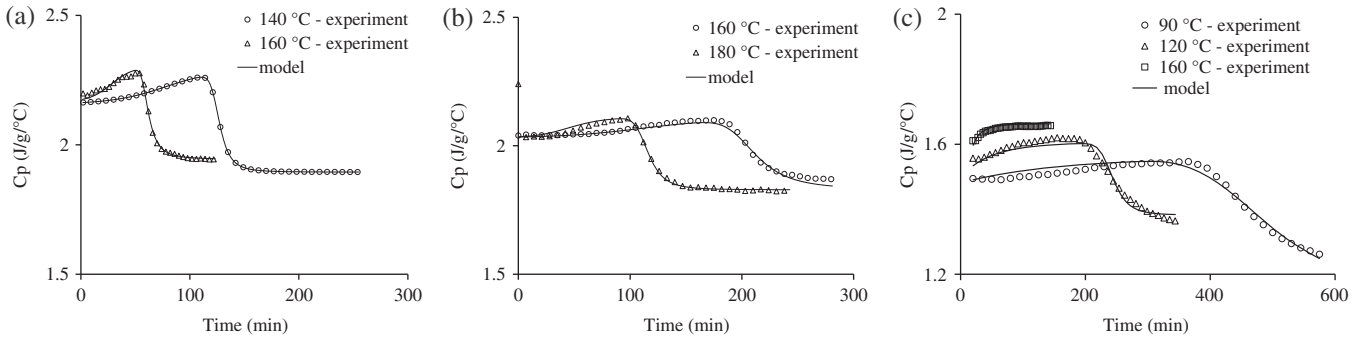

Figure 8. Specific heat capacity isothermal tests for (a) RTM6, (b) 890RTM, and (c) XU3508/XB3473.

Table IV. Specific Heat Capacity Model Parameters

	RTM6	890RTM	XU3508/XB3473
C_{rub}(J g^{-1} ◦ C^{-1})	2.10	2.03	1.36
C_{rubT} (J g^{-1} ◦ C^{-2})	4.19×10^{-4}	0.00	13.6×10^{-3}
$C_{rub\alpha}$ (J g^{-1} ◦ C^{-1})	0.16	0.081	0.080
C_{glass} (J g^{-1} ◦ C^{-1})	1.55	1.85	0.305
C_{glassT} (J g^{-1} ◦ C^{-2})	2.44×10^{-3}	-1.00×10^{-4}	8.97×10^{-3}
C_w (°C^{-1})	0.474	0.297	0.935
σ (°C)	107.6	401.5	74.0
σ_T	−0.454	−2.26	−0.714

Table V. Thermal Expansion Coefficient and Volumetric Shrinkage Parameters[22–24,32,34,35]

	RTM6	890RTM	XU3508/XB3473
ρ (kg m^{-3})	1110	1130	1150
α_{vr} (C^{-1})	0.000136	0.000125	0.00019
γ	0.054	0.088	0.083

The specific heat capacity values computed using eq. (17) and density values calculated using eq. (18) have been used to estimate the thermal conductivity evolution based on eq. (9) and the experimental lag estimated during tests. Among the three tests per condition, outliers have been rejected, and the average of the remaining tests has been calculated and reported in Figure 10 for RTM6, 890RTM, and XU3508/XB3473. Because of the nature of the thermal conductivity tests, the isothermal temperature is an average of the sinusoidal temperature given by the temperature controller. The aim was to have an average temperature similar to the temperatures used for the specific heat capacity characterization.

The results show a clear dependence of thermal conductivity on curing temperature. In particular, thermal conductivity decreases with increasing temperature for a given degree of cure. This trend, which is observed for all three systems of this study, is in agreement with results reported in the literature for different resin systems at temperatures above the glass transition[36,37] and can be attributed to increased phonon scattering and to loosening of interactions between molecules as a result of increased thermal motion at higher temperatures. In the case of the RTM6 resin, a 20 °C temperature increase results in a 25% drop in thermal conductivity. This sensitivity in the case of 890RTM is about 22% over a 20 °C increment. In the case of the XU3508/XB3473 system, the sensitivity is significantly lower at about 11% over a 20 °C increment. The dependence of thermal conductivity on the degree of cure also follows a common trend for the three epoxies of this study, with conductivity increasing as the reaction progresses.

Table VI. Estimated Thermal Conductivity Using the Data Reduction Procedure and Artificial Data Produced from the FE Simulation of Curing 890RTM Resin at Different Temperatures and with/without Heat Generation

	Without heat generation		With heat generation	
Temperature (°C)	K (W m^{-1}◦C^{-1})	Error (%)	K (W m^{-1}◦C^{-1})	Error (%)
160	0.1517	1.1	0.1512	0.8
180	0.1515	1.0	0.1517	1.2
200	0.1519	1.3	0.1519	1.3

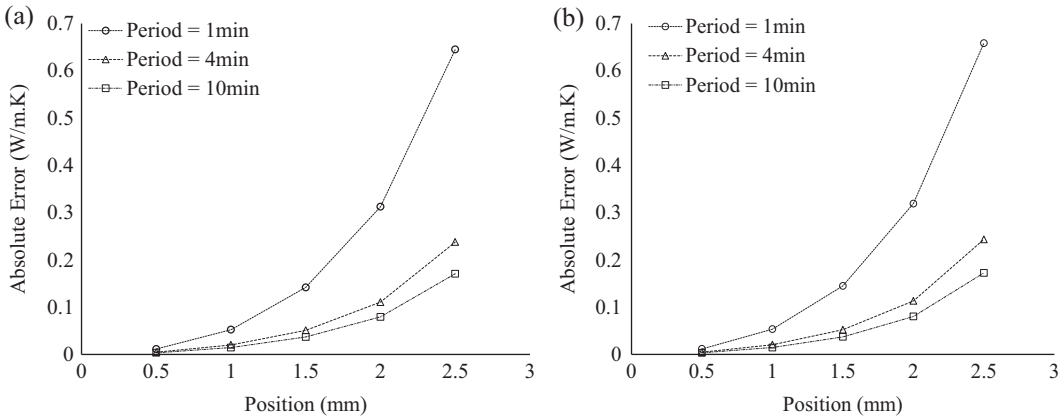

Figure 9. Parameter sensitivity analysis for (a) RTM6 and (b) 890RTM.

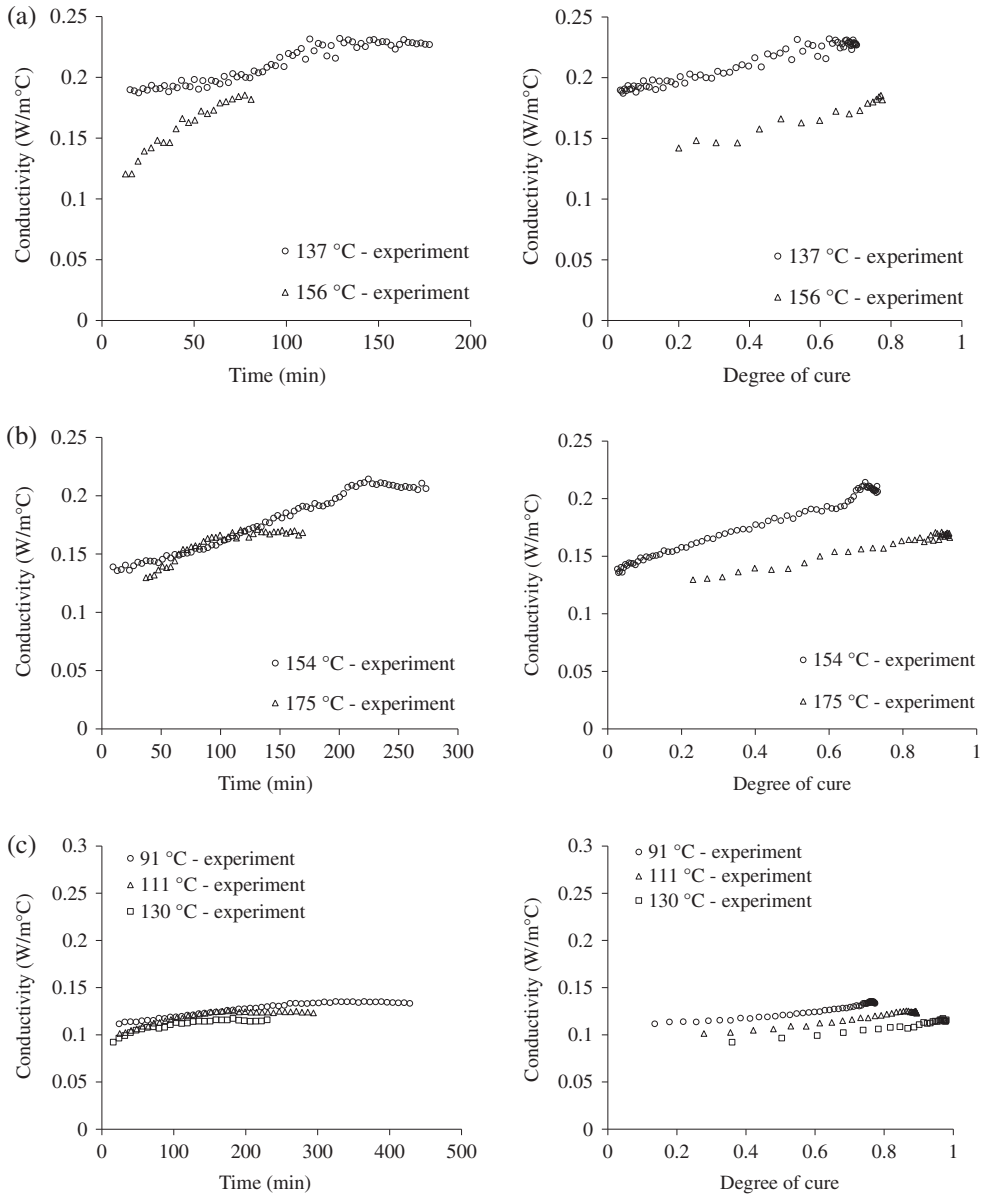

Figure 10. Thermal conductivity vs time and the degree of cure for (a) RTM6, (b) 890RTM, and (c) XU3508/XB3473.

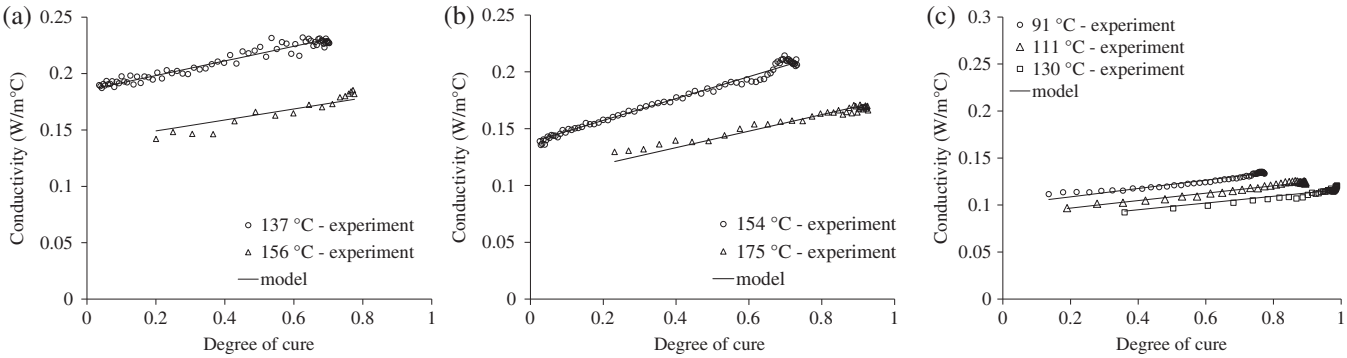

Figure 11. Thermal conductivity modeling for (a) RTM6, (b) 890RTM, and (c) XU3508/XB3473.

Table VII. Thermal Conductivity Model Parameters

	θ (W m^{-1} K^{-1})	β (W^{-1} m K)	γ (m W^{-1})
RTM6	0.35	−33.6	0.095
890RTM	0.70	−41.8	0.115
XU3508/XB3473	0.44	−12.1	0.061

[Corrections added on 13 November 2018 after first online publication: Table VII second column header text added, fourth column extended amounts to three decimals for accuracy.]

This behavior can be attributed to the tightening of the structure and the increased interaction between molecular groups as the crosslinking increases, facilitating phonon transport. In the case of RTM6, a 1% increase in the degree of cure results in a 0.3% increase in thermal conductivity, whereas for 890RTM and XU3508/XB3473, a 0.4% and 0.2% thermal conductivity increase is observed for the same degree of cure increment, respectively.

The thermal conductivity results obtained in this study can be modeled by introducing an inverse dependence on temperature[36,37] and a linear dependence on the degree of cure.[38,39] For dielectrics with no free electrical charges such as thermosets, phonons can be considered as the main heat carriers, and the thermal conductivity can be expressed using Matthiessen's rule with the addition of linear dependence on the degree of cure:

$$K = \frac{1+\theta\alpha}{\beta+\gamma T} \tag{19}$$

where θ is a fitting parameter controlling the linear dependence on the degree of cure, β is the contribution of structure scattering and of vacant-site scattering to thermal resistance, and γ is a fitting parameter governing the dependence on absolute temperature.

Figure 11 depicts the fitting of the experimental data with the model represented by eq. (19). The fitting parameter values are reported in Table VII.

It can be observed that for the two single-component systems, parameters β and γ are close. This indicates similarities of these materials in terms of microscopic structure, resulting in similar structural scattering behavior.

CONCLUSIONS

The method and apparatus developed in this study is compact and practical, while it is reliable in measuring thermal conductivity of liquid thermosets during their cure. The accuracy of the measurement is controlled by the accuracy of thermocouple placement at the center of the resin region. A positional accuracy of 0.5 mm is required to limit the measurement error below 3%. The thermal conductivity of curing epoxies shows a linearly increasing dependence on the degree of cure and an inversely linear dependence on temperature. The results obtained can be interpreted on the basis of phonon transport as the main heat carriers in the curing material. The experimental setup can be used to generate material characterization data necessary to build accurate thermal conductivity constitutive models for curing simulation. Measurement of the evolution of thermal conductivity during the cure can lead to more reliable predictions of thermal gradients, exothermic phenomena, and defects such as residual stresses contributing to enhancing the overall accuracy of predictive tools.

ACKNOWLEDGMENTS

This work was supported by the European Commission through the FP7 projects PULAERO (605613), the H2020 Clean Sky project SimCoDeQ (686493), and the Engineering and Physical Sciences Research Council, through the EPSRC Grant RPOACM (EP/K031430/1). Data underlying this study can be accessed through the Cranfield University repository at https://doi.org/10.17862/cranfield.rd.5841240.

CONFLICT OF INTEREST

The authors declare no conflict of interest.

REFERENCES

1. Farmer, J.; Covert, E. *J. Thermophys. Heat Transfer*. **1994**, *8*, 358.
2. Farmer, J.; Covert, E. *J. Thermophys. Heat Transfer*. **1996**, *10*, 467.
3. Bailleul, J. L.; Delaunay, D.; Jarny, Y.; Jurkowski, T. *J. Reinf. Plast. Compos.* **2001**, *20*, 52.
4. Garnier, B.; Sommier, A. *J. Reinf. Plast. Compos.* **2002**, *21*, 1193.
5. Friis-Pedersen, H.; Pedersen, J. H.; Haussler, L.; Storm, B. K. *Polym. Test.* **2006**, *25*, 1059.
6. Keating, M.; Mclaren, C. *Thermochim. Acta*. **1990**, *166*, 69.
7. Merzlyakov, M.; Schick, C. *Thermochim. Acta*. **2001**, *377*, 183.

8. Hu, M.; Yu, D.; Wei, J. *Polym. Test.* **2007**, *26*, 333.
9. Cecen, V.; Tavaman, I. H.; Kok, M.; Aydogdu, Y. *Polym. Compos.* **2009**, *30*, 1299.
10. Iguchi, C.; dos Santos, W. N.; Gregorio, R. *Polym. Test.* **2007**, *26*, 788.
11. dos Santos, W. N.; Mummery, P.; Wallwork, A. *Polym. Test.* **2005**, *24*, 628.
12. dos Santos, W. N. *Polym. Test.* **2007**, *26*, 556.
13. McHugh, J.; Stark, W. *Polym. Test.* **2016**, *49*, 115.
14. Lobo, H.; Cohen, C. *Polym. Eng. Sci.* **1990**, *30*, 65.
15. Zhang, X.; Fujii, M. *Polym. Eng. Sci.* **2003**, *43*, 1755.
16. Zhang, X.; Hendro, W.; Fujii, M.; Tomimura, T.; Imaishi, N. *Int. J. Thermophys.* **2002**, *23*, 1077.
17. dos Santos, W. N. *Polym. Test.* **2005**, *24*, 932.
18. Scott, E.; Beck, J. *J. Compos. Mater.* **1992**, *26*, 20.
19. Skordos, A. A.; Partridge, I. K. *Inverse Probl. Sci. Eng.* **2004**, *12*, 157.
20. Carslaw, H. S.; Jaeger, J. C. Conduction of Heat in Solids; UK: Oxford University Press, **1959**.
21. Sigma-Aldrich®. www.sigmaaldrich.com (accessed May 2018).
22. Hexcel®. www.hexcel.com (accessed May 2018).
23. Cycom®. www.cytec.com (accessed May 2018).
24. Huntsman®. www.huntsman.com (accessed May 2018).
25. Marc®, Volume A. www.mscsoftware.com (accessed May 2018).
26. Marc®, Volume B. www.mscsoftware.com (accessed May 2018).
27. Marc®, Volume D. www.mscsoftware.com (accessed May 2018).
28. van Gelder, M. F. Ph.D. Thesis, Virginia Tech, **1998**.
29. Karkanas, P. I.; Partridge, I. K. *J. Appl. Polym. Sci.* **2000**, *77*, 1419.
30. Khoun, L.; Centea, T.; Hubert, P. *J. Compos. Mater.* **2010**, *44*, 1397.
31. Pascault, J. P.; Williams, R. J. J. *J. Polym. Sci.* **1990**, *28*, 85.
32. Svanberg, J. M.; Altkvist, C. *J. Reinf. Plast. Compos.* **2005**, *24*, 323.
33. Struzziero, G.; Skordos, A. A. *Composites Part A*. **2017**, *93*, 126.
34. PUL-AERO project, Seventh Framework Programme. www.pul-aero.eu (accessed May 2018).
35. Khoun, L.; Hubert, P. *Polym. Compos.* **2010**, *31*, 1603.
36. Dashora, P.; Gupta, G. *Polymer*. **1996**, *37*, 231.
37. Dashora, P. *Phys. Scr.* **1994**, *49*, 611.
38. Yamamoto, O. *Polym. J.* **1971**, *2*, 509.
39. Yamamoto, O.; Kambe, H. *Polym. J.* **1971**, *2*, 623.

2018-08-28

Measurement of thermal conductivity of epoxy resins during cure

Struzziero, G.

Wiley

Struzziero G, Remy B, Skordos AA. (2019) Measurement of thermal conductivity of epoxy resins during cure. Journal of Applied Polymer Science, Volume 136, Issue 5, February 2019, Article number 47015

https://doi.org/10.1002/app.47015